CONVERSION OF SELECTIVE CHARACTERISTICS OF ELECTRICALLY CONTROLLED CHIRPED MULTILAYER INHOMOGENEOUS DIFFRACTION STRUCTURES BASED ON PHOTOPOLYMERIZING COMPOSITIONS WITH NEMATIC LIQUID CRYSTALS

© 2025 S. N. Sharangovich, V. O. Dolgirev, D. S. Rastrygin*

Tomsk State University of Control and Radioelectronics Systems, Tomsk, Russia

**e-mail: gg9dragon9gg@gmail.com*

Received September 06, 2024

Revised September 16, 2024

Accepted September 30, 2024

Abstract. We developed the analytical model of optical radiation diffraction on chirped multilayer inhomogeneous diffraction structures formed by the holographic method in photopolymerizing compositions with nematic liquid crystals having smooth optical heterogeneity in layer thickness. By numerical calculation, it was shown that using the chirping method it is possible to multiply the angular and spectral characteristics of multilayer inhomogeneous holographic diffraction structures formed in photopolymerizing compositions with nematic liquid crystals.

Keywords: *multilayer inhomogeneous diffraction structures, photopolymerizing compositions with nematic liquid crystals, chirped structures*

DOI: 10.31857/S03676765250105e7

INTRODUCTION

In modern science, there is a growing interest in multilayer inhomogeneous holographic diffraction structures (MNHDS). These structures have the potential to be widely used as key components in optical communication networks as multiplexers [1-7] and in the generation of femtosecond laser pulses [8-13]. The main feature of such structures is their angular selectivity, which manifests itself in the formation of a set of local maxima that depend on the ratio of the thicknesses of intermediate and diffraction layers.

Earlier studies [1, 2] demonstrated the prospect of controlling the angular selectivity of both single and multiplexed MNGDS formed in photopolymer compositions containing high concentrations of nematic liquid crystals (FPM-LCs). For example, the application of an external electric field to certain diffraction layers allowed not only to change the level of diffraction efficiency, but also to modify the angular response itself, accompanying this process with a significant shift in angular selectivity [2]. In the case of multiplexed MNGDS, where several diffraction structures at different recording angles were sequentially formed, a multiple expansion of both angular and spectral characteristics was observed [1].

At the same time, broadening of angular and spectral characteristics for photonic structures is also possible by changing the period along the lattice vector (chirping). Thus, for example, in [14], the authors showed on the example of single holographic diffraction structures (HDS) in FPM the possibility of broadening the selective response of diffracted radiation due to the formation of a structure with a changing period.

Thus, the main objective of this work is to investigate the conversion process of selective performance of electrically controlled chirped FPM-LC based MNGDS.

THEORETICAL PART

The mathematical model of diffraction of optical radiation on chirped MNGDS with FPM-LC, is developed according to [2].

To create chirped MNGDS, two monochromatic light beams with different phase characteristics are used. One of the beams has a constant phase distribution E_0 , while the other beam is characterized by phase inhomogeneities E_1 . These two waves are aimed at the complex multilayer FPM-LC structure at angles θ_0 and θ_1. In this case, the phase profile $\varphi_c^n(\vec{r})$ of the chirped structure for each layer will be taken into account [14]:

$$\varphi_c^n(\vec{r}) = \varphi_0^n + \nabla\varphi^n \cdot \vec{r} + 0{,}5\nabla^2\varphi^n \cdot \vec{r}^{\,2}, \qquad (1)$$

where $\nabla\varphi^n = K_0^n$ is the mean and $0.5\nabla^2\varphi^n$ is the quadratic coefficient of variation of the modulus of the lattice vector $\vec{K}$.

The dielectric permittivity tensor for FPM-LC in the *n-th* layer of MNGDS with variable period will be determined by the following parameters: the LC volume fraction, the variation of the polymer and LC component composition, and the chirped structure itself:

$$\hat{\varepsilon}^n = (1-\rho)(\varepsilon_p^n \cdot \hat{I} + \Delta\hat{\varepsilon}_c^n + \Delta\hat{\varepsilon}_p^n) + \rho(\hat{\varepsilon}_{LC}^n + \Delta\hat{\varepsilon}_c^n + \Delta\hat{\varepsilon}_{LC}^n), \qquad (2)$$

where ρ - defines the volume fraction of nematic LC, $\hat{\mathrm{I}}$ - unit tensor, ε_p^n - value of the polymer component, $\hat{\varepsilon}_{LC}^n$ - dielectric tensor of the LC component, $\Delta\hat{\varepsilon}_p^n$ and $\Delta\hat{\varepsilon}_{LC}^n$ - functions defining the variation of the dielectric tensor, $\Delta\hat{\varepsilon}_{\mathrm{c}}^n = 0.5\Delta\hat{\varepsilon}_p^n\left[U_0 U_m(\vec{r})\exp\left(i\cdot\varphi_{\mathrm{c}}^n(\vec{r})\right)\right]$ - periodic variations in the dielectric tensor, U_0 and U_m - amplitude of the dielectric perturbation and normalized amplitude profile.

When solving the diffraction problem, let us assume that the light beam $\vec{E}^0$, incident on the MNGDS, has an arbitrary polarization with a unit complex polarization vector $\vec{e}_0$ (Fig. 1). In the case of Bragg diffraction of light in optically inhomogeneous FPM-LC layers, we can use the method of slowly varying amplitudes and determine the amplitudes of interacting waves using a system of coupled wave equations in partial derivatives of the following form [1, 2]:

$$\begin{aligned}\vec{N}_{\mathrm{r}0}^{m,n}\cdot\nabla E_0^{m,n} &= -iC_1^{m,n}\cdot n_1^{m,n}\cdot E_1^{m,n}\cdot\exp\left[+i\Theta^{m,n}\right],\\ \vec{N}_{r1}^{m,n}\cdot\nabla E_1^{m,n} &= -iC_0^{m,n}\cdot n_1^{m,n}\cdot E_0^{m,n}\cdot\exp\left[-i\Theta^{m,n}\right],\end{aligned} \tag{3}$$

where $C_j^{m,n}\left(\vec{E}\right)=\omega\left(\vec{e}_1^{\,m,n}\Delta\varepsilon^n(\vec{r})\vec{e}_0^{\,m,n}\right)(c_c n_{1,0}^{m,n}\cos\beta_{1,0}^{m,n})^{-1}/4$ are the coupling coefficients, $j=\{0,1\}$ is the diffraction order, $\vec{r}$ is the radius vector, $n=1...N$ is the number of diffraction layers, N is the number of the last layer, $m=\mathrm{o,e}$ is the index corresponding to ordinary and extraordinary waves, $n_1^{m,n}$ determines the normalized refractive index profile of the first harmonic of the GDS, $\Theta^{m,n}\left(\vec{r},\vec{E}\right)$ is the integral phase disorder parameter, which is expressed as [1, 2]:

$$\Theta^{m,n}(\vec{r},\vec{E})=\int_0^{\vec{r}}\Delta\vec{K}^{m,n}\left(\vec{r}_i,\vec{E}\right)d\vec{r}_i\,, \tag{4}$$

The integral phase disorder $\Theta^{m,n}\left(\vec{r},\vec{E}\right)$ is a parameter with a complex dependence, which in turn complicates the process of obtaining solutions for the coupled-wave equations at high diffraction efficiency [1, 2]. However, a solution can still be found if one approximates $\Theta^{m,n}\left(\vec{r},\vec{E}\right)$ by a parabolic function for each FPM-LC layer, as was shown in [1, 2]. Thus, there arises a coupling between the layers, which is given by the parameter $\Theta^{m,n-1}$.

In the case of the near diffraction zone (Fig. 1), the light field expressions for the zero and first diffraction order at the output of the chirped MNGDS can be defined as [1, 2]:

$$\begin{aligned} \vec{E}_1^n(\eta) &= \vec{e}_1^{\,o,n} E_1^{o,n}(\eta)\exp[-i\int_0^{d_n}\vec{k}_1^{o,n} d\vec{r}_i] + \vec{e}_1^{\,e,n} E_1^{e,n}(\eta)\exp[-i\int_0^{d_n}\vec{k}_1^{e,n} d\vec{r}_i], \\ \vec{E}_0^n(\xi) &= \vec{e}_0^{\,o,n} E_0^{o,n}(\xi)\exp[-i\int_0^{d_n}\vec{k}_0^{o,n} d\vec{r}_i] + \vec{e}_0^{\,e,n} E_0^{e,n}(\xi)\exp[-i\int_0^{d_n}\vec{k}_0^{e,n} d\vec{r}_i], \end{aligned} \tag{5}$$

where $\xi_0 = \xi$, $\xi_1 = \eta$, ξ_0, ξ_1 are aperture coordinates.

To find the diffraction field distribution in the far diffraction zone, it is necessary to take advantage of the relationship between the spatial distributions and angular spectra of the diffracting beams [1, 2]:

$$E_j^m(\theta) = \int_{-\infty}^{\infty} E_j^m(l)\exp\left[ik_j^m l\theta\right]dl, \tag{6}$$

where the angle θ defines the orientation of the plane-wave components of $E_j^m(\theta)$ with respect to the wave normals, and $l = \xi_0, \xi_1$.

Then, using the matrix method, we can describe the transformation process of the frequency-angle spectra of interacting plane light waves through the whole multiplexed MNGDS [1, 2]:

$$\vec{E}^{m,N} = \vec{T}^{m,N} \cdot \vec{A}^{m,N-1} \cdot \vec{T}^{m,N-1} \cdot \ldots \cdot \vec{A}^{m,1} \cdot \vec{T}^{m,1} \cdot \vec{E}^{0}, \tag{7}$$

where $\vec{E}^{m,N} = \begin{bmatrix} E_0^{m,N}(\omega,\Delta K) \\ E_1^{m,N}(\omega,\Delta K) \end{bmatrix}$, $\vec{T}^{m,n,n_h} = \begin{bmatrix} T_{00}^{m,n,n_h}(\omega,\Delta K) & T_{10}^{m,n,n_h}(\omega,\Delta K) \\ T_{01}^{m,n,n_h}(\omega,\Delta K) & T_{11}^{m,n,n_h}(\omega,\Delta K) \end{bmatrix}$ is the matrix transfer function for the nth FPM-LC layer, $\vec{E}^{0} = \begin{bmatrix} E_0(\omega,\Delta K) \\ 0 \end{bmatrix}$, ω is the frequency of the reading beam, ΔK is the phase disorder, $\vec{A}^{m,n}$ is the transition matrix for the buffer layer [8].

The components of the matrix $\vec{T}^{m,n}$ are defined as [1, 2]:

$$T_{00}^{m,n} = -\frac{C_0^{m,n} C_1^{m,n} d_n^2}{4\nu_1\nu_0} \int_{-1}^{+1} \exp\left[\delta m'(1-y) + \delta^2 n'(1-y)^2\right] \cdot$$
$$\cdot \Phi\left(\frac{d'}{b'} + 1, 2; b'\delta^2 \frac{\nu_1}{\nu_0}(1-y^2)\right) dy,$$

$$T_{10,01}^{m,n} = -i\frac{C_{1,0}^{m,n} d_n}{2\nu_{0,1}} \int_{-1}^{+1} \exp\left[\delta m'(1-y) + \delta^2 n'(1-y)^2\right] \times \Phi\left(\frac{d'}{b'}, 1; b'\delta^2 \frac{\nu_1}{\nu_0}(1-y^2)\right) dy,$$

$$T_{11}^{m,n} = -\frac{C_0^{m,n} C_1^{m,n} d_n^2}{4\nu_1\nu_0} \int_{-1}^{+1} \exp\left[\delta m(1-y) + \delta^2 n(1-y)^2\right] \cdot$$
$$\cdot \Phi\left(\frac{d'}{a} + 1, 2; a\delta^2 \frac{\nu_1}{\nu_0}(1-y^2)\right) dy,$$

where Φ $(a,b;c)$ is a degenerate hypergeometric function of the first kind, , $\delta = d_n\left(\eta_1\nu_0 - \eta_0\nu_1\right)/2\nu_1$ $\theta_{rj}^{m,n}$ are the angles between the group normals $\vec{N}_{rj}^{m,n}$ and the y-axis, $\eta_j = \eta_j^{m,n} = \pm\sin\theta_{rj}^{m,n}$, $m = \eta\left(-a + b\nu_1/\nu_0\right) - i\Delta K' d_n / 2\delta$, $\nu_j = \nu_j^{m,n} = \cos\theta_{rj}^{m,n}$,

$$d' = -\sigma^2, \qquad m' = \xi\left(-a'/2 + b'\nu_1/\nu_0\right) - i\Delta K' d_n / 2\delta, \qquad a' = -i\frac{t_y^{n2}\nu_1}{\left(\eta_1\nu_0 + \eta_0\nu_1\right)^2},$$

$$a = i\frac{t_y^n \nu_1 \nu_0}{\left(\eta_1\nu_0 + \eta_0\nu_1\right)^2}, \qquad n' = \frac{b'\nu_1}{\nu_0} - \frac{a'}{2}, \qquad b = i\frac{t_y^n \nu_0^2}{\left(\eta_1\nu_0 + \eta_0\nu_1\right)^2}, \qquad n = \frac{\nu_1}{\nu_0}\left(a - \frac{b\nu_1}{2\nu_0}\right),$$

$$b' = -i\frac{t_y^n \nu_1 \nu_0}{\left(\eta_1\nu_0 - \eta_0\nu_1\right)^2}, \quad \sigma = \frac{C_0^{m,n} C_1^{m,n}}{\left(\eta_1\nu_0 - \eta_0\nu_1\right)^2} .$$

In the case of light diffraction on non-chirped MNGDS formed in FPM without LC having homogeneous refractive index profiles, components of the matrix $\vec{T}^{m,n}$ go to the known ones obtained by other authors [5, 6].

NUMERICAL CALCULATION

In numerical modeling, a two-layer GDS with homogeneous refractive index profiles was investigated, in which a chirped diffraction structure was recorded at a wavelength of $\lambda = 633$ nm and angles between the recording beams $2\theta = 16$ degrees. Parameters for modeling: $\lambda_{\text{read}} = 1431$ nm is the reading wavelength; $d_n = 20$ μm is the thickness of the FPM-LC layers; $t_n = 120$ μm is the thickness of the intermediate layer; the Bragg angle for the (λ_{read}) reading wavelength is $\theta_b = 18$ degrees.

Figure 2 shows the dependence of diffraction efficiency (η) on the rotation angle and readout wavelength of both single and bilayer GDSs, which had both a constant grating period and varied with a quadratic coefficient $0.5\nabla^2\varphi^n = 3\cdot 10^5$.

As can be seen from Figure 2, the presence of a changing period in the GDS leads to a broadening of the angular and spectral characteristics by a factor of 3.6 compared to the standard GDS. If we compare the obtained data with the results for multiplexed

MNGDS from [1, 2], then in the case of multiplexed MNGDS the increase in angular and spectral characteristics was realized due to the merging of the selectivities of two gratings, while the width of local maxima did not change and their number increased. For the case with chirped MNGDS, the number of local maxima remains unchanged, but their width increases. Thus, for constancy of the width of local maxima in the case of chirped MNGDS it is necessary to increase the width of the buffer layer.

Figure 3 shows the dependence of the diffraction efficiency of the two-layer standard and chirped GDS on the rotation angle and readout wavelength when an external electric field is applied to each photopolymer layer with liquid crystals.

As can be seen from Figure 3, at external electric influence to each diffraction layer there is a decrease in diffraction efficiency and a shift of angular selectivity at reading by light radiation with polarization coinciding with the intrinsic extraordinary waves in the sample by the same value, which directly depends on the thickness of the diffraction layer. At the same time, the offset is more significant for the standard MNGDS with respect to the total width of the angular selectivity than for the chirped structure. For example, at electric field strength $E = 1.16E_c$, where $E_c$is the Fredericks critical strength [15], the shift for the standard MNGDS amounted to 5 local maxima, while for the chirped one - 2.

Figure 4 shows the dependence of the diffraction efficiency of the two-layer standard and chirped GDS on the rotation angle and the readout wavelength when read by a light wave with a polarization angle of 30 degrees and an electric voltage on the diffraction layers $E = 1.32E_c$.

As can be seen from Figure 4, at electric influence and reading by a light wave, the polarization of which differs from its own extraordinary waves in the sample, the diffraction of light occurs both on ordinary waves and on extraordinary waves. At the same time, for extraordinary waves is characterized by a shift in the angular selectivity, due to the influence of the electric field, and for ordinary waves there is no shift. In turn, for standard MNGDS, a significant increase in the number of local maxima can be observed due to the superposition of the angular selectivities on ordinary and extraordinary waves. For chirped MNGDS, this effect is less noticeable due to the insignificant shift of the angular selectivity with respect to the width of the local maxima.

CONCLUSION

Thus, we have investigated the transformation of selective characteristics of electrically controlled chirped multilayer inhomogeneous holographic diffraction structures formed in photopolymer compositions with a high content of nematic liquid crystals. It is found that at reading of chirped multilayer heterogeneous holographic FPM-LC diffraction structures the number of local maxima of angular selectivity remains unchanged, but their width increases. When reading the chirped multilayer inhomogeneous holographic FPM-LC diffraction structures by a light wave, the polarization of which coincides with the polarization of its own extraordinary waves, and at the same polarity of the applied external electric field to each diffraction layer there is a decrease in diffraction efficiency with a shift of angular selectivity to one side. At the same time, relative to the total width of the angular selectivity, in the chirped structure the shift occurs at a smaller number of local maxima, due to their significant broadening. When reading the chirped multilayer inhomogeneous holographic FPM-LC diffraction structures by a light wave, the polarization of which does not coincide with the polarization of its own extraordinary waves, and with the same polarity of the applied external electric field to each diffraction layer, the number of local maxima can be increased due to the diffraction of light on ordinary and extraordinary waves. At the same time, the increase in the number of local maxima in the chirped structure will be lower compared to the standard structure, which is due to the insignificant shift of the angular selectivity of diffracted radiation on ordinary waves relative to the width of local maxima.

It is demonstrated that the chirping method can be used to multiply the angular and spectral characteristics of multilayer inhomogeneous holographic diffraction structures formed in photopolymerizing compositions with nematic liquid crystals.

REFERENCES

1. *Sharangovich S.N., Dolgirev V.O., Rastrygin D.S.* // Bull. Russ. Acad. Sci. Phys. 2024. V. 88. No. 1. P. 6.

2. *Sharangovich S.N., Dolgirev V.O.* // Bull. Russ. Acad. Sci. Phys. 2023. V. 87. No. 1. P. 7.

3. *Malallah R., Li H., Qi Y. et al.* // J. Opt. Soc. Amer. A. 2019. V. 36. No. 3. P. 320.

4. *Malallah R., Li H., Qi Y. et al.* // J. Opt. Soc. Amer. A. 2019. V. 36. No. 3. P. 334.

5. *Pen E.F., Rodionov M.Yu., Chubakov P.A.* // Optoelectron. Instrum. Data Process. 2017. V. 53. P. 59.

6. *Pen E.F., Rodionov M.Yu. //* Quantum Electron. 2017. V. 40. No. 10. P. 919.

7. *Nordin G.P., Johnsonm R.V. //* J. Opt. Soc. Amer. A. 1992. V. 9. No. 12. P. 2206.

8. *Yan X., Wang X., Chen Y. et al.* // Appl. Phys. B. 2019. V. 125. Art. No. 67.

9. *Yan X., Gao L., Yang X. et al.* // Opt. Express. 2014. V. 22. No. 21. P. 26128.

10. *Kazanskiy N.L., Khonina S.N., Karpeev S.V. et al.* // Quantum Electron. 2020. V. 50. No. 7. P. 629.

11. *Kudryashov S.I.* // Appl. Surf. Sci. 2019. V. 484. P. 948.

12. *Pavlov D.* // Optics Lett. 2019. V. 44. No. 2. P. 283.

13. *Aimin Y., Liren L., Yanan Z. et al. //* J. Opt. Soc. Amer. A. 2009. V. 26. No. 1. P. 135.

14. *Dovolnov E.A., Sharangovich S.N., Sheridan J.T.* // Photorefractive effects, materials, and devices 2005 (PR05). OSA Trends in Optics and Photonics Series (TOPS), 2005. P. 337.

15. *Sonin A.S.* Introduction to the Physics of Liquid Crystals. M.: Nauka. Glavn. ed. fiz.-mat. litt., 1983. 320 c.

FIGURE CAPTIONS

Fig. 1. Schematic of light diffraction on electrically controlled period-varying MNGDS in FPM-LC**.**

Fig. 2. Dependence of diffraction efficiency on rotation angle and readout wavelength.

Fig. 3. Dependence of diffraction efficiency on the rotation angle and readout wavelength when exposed to an external electric field.

Fig. 4. Dependence of diffraction efficiency on the rotation angle and readout wavelength when exposed to an external electric field and the polarization angle of the readout radiation θ = 30 degrees.

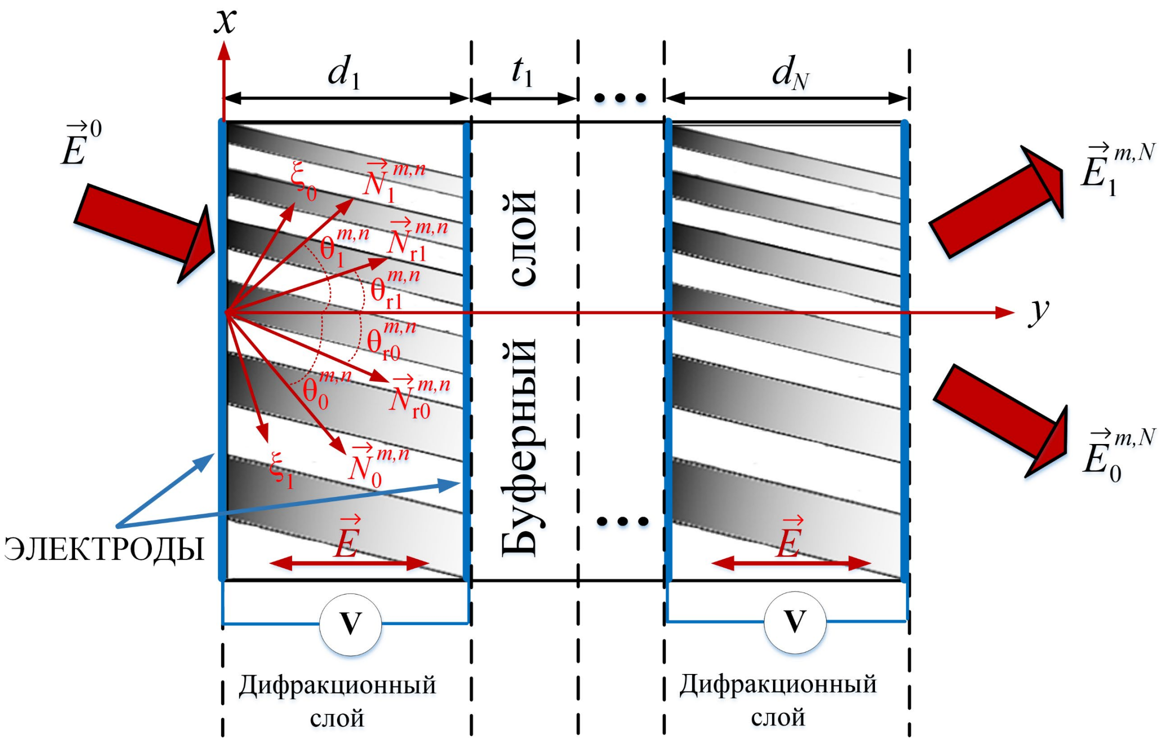
x
d1
t1
dN
E0
E1 m,N
E0 m,N
y
ξ0
ξ1
N1 m,n
Nr1 m,n
Nr0 m,n
N0 m,n
θ1 m,n
θr1 m,n
θr0 m,n
θ0 m,n
Буферный слой
ЭЛЕКТРОДЫ
E
V
Дифракционный слой
Дифракционный слой

Fig. 1.

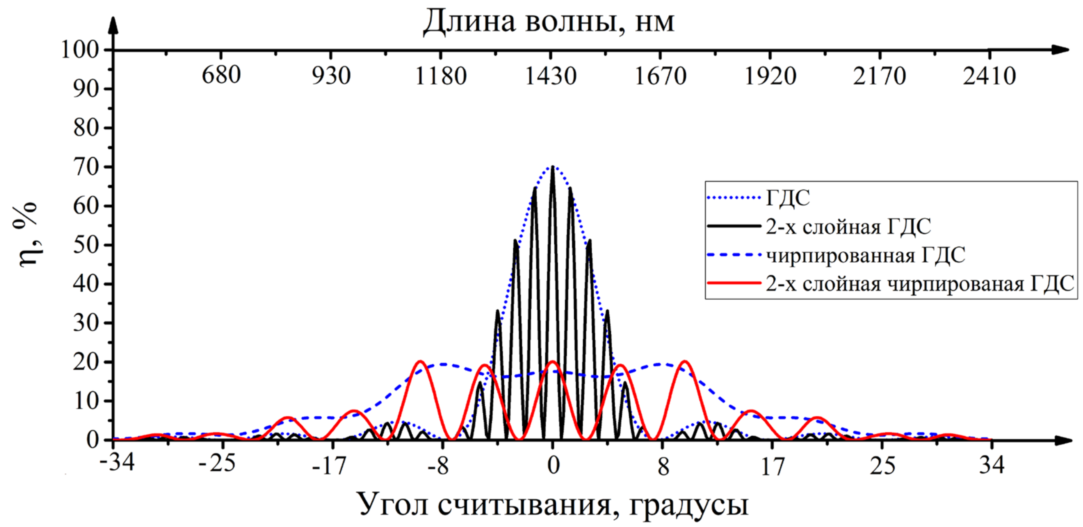
Длина волны, нм
680
930
1180
1430
1670
1920
2170
2410
η, %
100
90
80
70
60
50
40
30
20
10
0
ГДС
2-х слойная ГДС
чирпированная ГДС
2-х слойная чирпированая ГДС
-34
-25
-17
-8
0
8
17
25
34
Угол считывания, градусы

Fig. 2

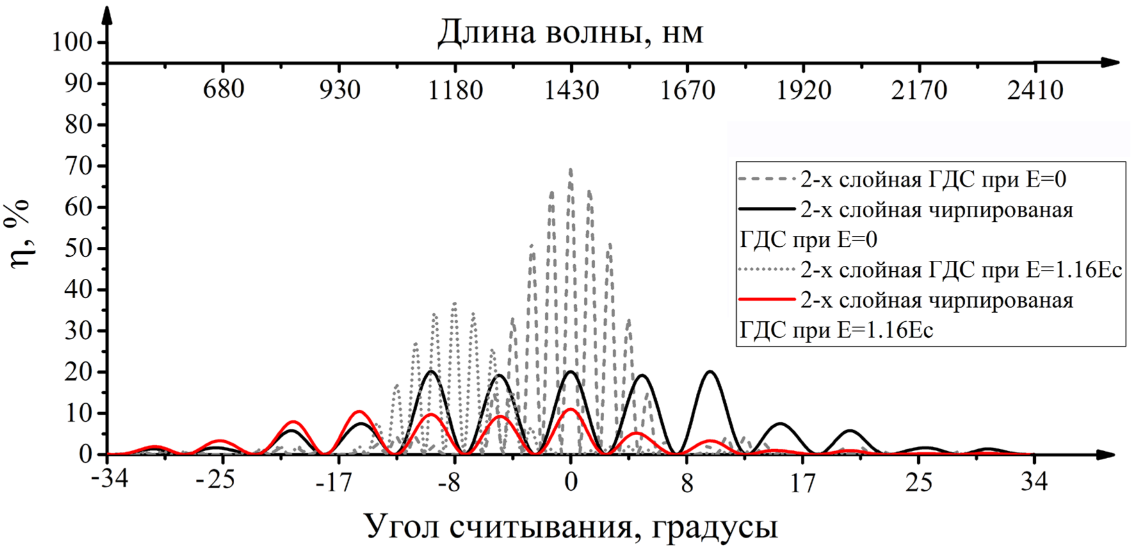
Длина волны, нм
680
930
1180
1430
1670
1920
2170
2410
η, %
100
90
80
70
60
50
40
30
20
10
0
2-х слойная ГДС при E=0
2-х слойная чирпированая ГДС при E=0
2-х слойная ГДС при E=1.16Ec
2-х слойная чирпированая ГДС при E=1.16Ec
-34
-25
-17
-8
0
8
17
25
34
Угол считывания, градусы

Fig. 3

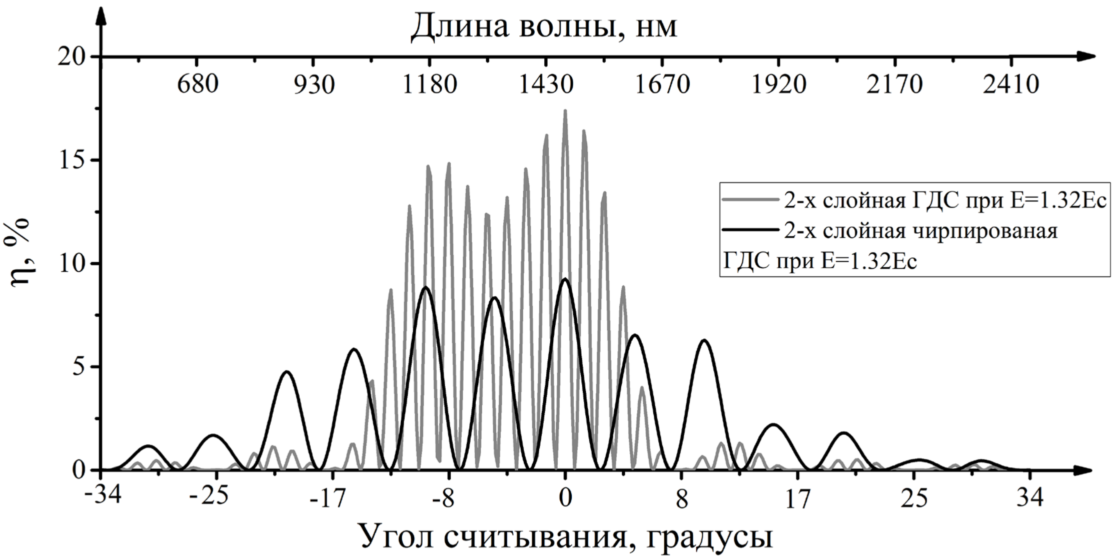
Длина волны, нм
680
930
1180
1430
1670
1920
2170
2410
η, %
20
15
10
5
0
2-х слойная ГДС при E=1.32Ec
2-х слойная чирпированая ГДС при E=1.32Ec
-34
-25
-17
-8
0
8
17
25
34
Угол считывания, градусы

Fig. 4